https://doi.org/10.3311/PPci.22430

Periodica Polytechnica Civil Engineering, 68(1), pp. 131–140, 2024

Prediction of Restrained Shrinkage of New-to-old Concrete Interface

Huili Wang[1*], Dequan An[1], Feng Nie[1], Hangshuai Zhao[2], Chunli Xu[3]

[1] National & Local Joint Engineering Laboratory of Bridge and Tunnel Technology, Dalian University of Technology, 116023 Dalian, China
[2] T. Y. Lin International Engineering Consulting Co., Ltd, 401120 Chongqing, China
[3] Shanghai Baoye Construction Corp., LTD, 200436 Shanghai, China
[*] Corresponding author, e-mail: wanghuili@dlut.edu.cn

Received: 18 April 2023, Accepted: 04 August 2023, Published online: 11 September 2023

Abstract

The focus of this study is on the shrinkage differences between new and old concrete, which can cause cracks at the bonding surface of the interface. The effects of various factors on shrinkage, such as the content of shrinkage reducing admixtures (SRA) the content of basalt fibers (BF) and the roughness at the new-to-old concrete interface (RI) are also examined. In this research, nine groups old-new concrete composite specimens were tested for shrinkage to gather experimental data. The restrained shrinkage mechanical model (RSMM) was deduced, and the restrained shrinkage model based on grey correlation analysis (RMGC) was proposed. The effectiveness and convenience of both prediction methods were evaluated by comparing their results to the experimental data. It was determined that the RMGC was more effective and convenient. Additionally, the research found that as the content of SRA and BF increases, shrinkage decreases. The effect of SRA was found to be more significant. As RI increases, shrinkage undergoes an initial increase and then decreases. The study can be used to inform the design and construction of structures that use both new and old concrete.

Keywords

shrinkage, old-new concrete, grey correlation analysis, test

1 Introduction

Long-term exposure to loads and environmental conditions in concrete structures, such as roads, bridges, airport runways, and dams, can lead to significant concrete shedding and cracking, posing a threat to their structural integrity. Therefore, it is essential to remove and replace damaged concrete with new material to ensure the ongoing stability of these structures. However, practical applications often encounter a discrepancy in shrinkage between the new and old concrete, resulting in cracks at the bond interface. The shrinkage of repair material cannot proceed freely due to the restraint provided by the substrate at interface. Typically, the shrinkage of the old concrete stabilizes over time, thereby restraining the shrinkage of the new concrete and inducing tensile stress within it. This results in the development of stress concentration at the interface, leading to a premature failure of repair overlay [1, 2]. Interfacial failure is generally caused by incompatibility due to the difference in shrinkage strain between the old concrete substrate and the newly applied concrete [3, 4]. Cracks may form when the tensile stress exceeds the tensile strength of the new concrete or the bond strength between the new and old concrete.

The behavior of concrete is significantly influenced by the occurrence of cracks caused by shrinkage [5]. Cracking problems associated with shrinkage are the topmost threat to the durability and safety of concrete today. In order to mitigate shrinkage and reduce the issues stemming from cracking, researchers have proposed several methods, including internal curing, modification of cement mix proportions, utilization of expansive agents or fibers, among others [6–8]. These approaches aim to control shrinkage and enhance the overall durability and safety of concrete.

This study builds upon previous research on the bonding performance of old-new concrete, which has been investigated by scholars in various aspects [9–14]. The content of SRA plays a crucial role in the shrinkage of old-new concrete [15–18]. SRA is widely used technology to reduce drying shrinkage and subsequent cracking of concrete [19].

Cite this article as: Wang, H., An, D., Nie, F., Zhao, H., Xu, C. "Prediction of Restrained Shrinkage of New-to-old Concrete Interface", Periodica Polytechnica Civil Engineering, 68(1), pp. 131–140, 2024. https://doi.org/10.3311/PPci.22430

SRA reduces the water surface tension stored inside the concrete pores, which is the primary mechanism of shrinkage [20]. Qin et al. [21] specifically examined the impact of SRA on the interfacial fracture roughness of the new-to-old concrete interface and observed an increase in interfacial fracture roughness when such admixtures were incorporated into the design mix of new concrete. Additionally, the addition of fibers has also shown potential in reducing the shrinkage of old-new concrete [22–24]. Cheng and Ga [25] conducted shrinkage experiments to identify the key factors influencing the adhesion between new steel fiber-reinforced concrete and old concrete. Yousefieh et al. [26] evaluated the performance of different fibers in reducing drying shrinkage and cracking under restrained conditions. Besides, the RI has been recognized as a factor affecting shrinkage [16, 27]. Santos and Júlio [28] assessed the influence of differential shrinkage on the bond strength of new-to-old concrete interfaces and investigated the behavior of RC composite members considering surface roughness, differential shrinkage, and stiffness experimentally. Furthermore, Lampropoulos and Dritsos [29] developed an analytical procedure to calculate the stresses induced by shrinkage in new concrete, considering a variable modulus of elasticity over time and relaxation due to creep. Wang et al. [30] conducted research on the long-term bonding behavior of prestressed old-new concrete composite beams under sustained loads. Beushausen and Alexander [2] and Beushausen and Bester [23] discussed the parameters that influence the bond strength between concretes of different ages using innovative experimental methods [31]. Mahsa found that surface moisture may increase the water-to-cement ratio, thereby potentially increasing the shrinkage of concrete [32].

The purpose of this study is to investigate the shrinkage in the new-to-old concrete interface. The effects of SRA, BF and RI were studied through experiments. The restrained shrinkage mechanical model (RSMM) and the restrained shrinkage model based on the grey correlation analysis (RMGC) at the new-to-old concrete interface were established. A comparison of the results obtained from the experiment with the results obtained using RSMM and RMGC was presented. The findings from this research can provide valuable information on the constrained shrinkage at the interface of old-new concrete and can inform the design and construction of structures that use both new and old concrete.

2 Experiment

2.1 Material

(1) *Concrete*

The concrete mix proportion used in the study is presented in Table 1. The type of cement used was P.O 42.5. The technique data of cement are listed in Table 2. The granularity of crushed stone is 5~25 mm. The grain size distribution curve is shown in Fig. 1. The fine aggregate uses river sand with a fineness modulus of 2.58.

(2) *Shrinkage reducing admixtures*

SRA used in the study is composed mainly of alkyl polyether. This is a type of chemical admixture that can be added to concrete to reduce the amount of shrinkage that occurs as the concrete dries and cures.

(3) *Basalt fiber*

BF is a type of silicate fiber, characterized by its high strength and temperature resistance. The average length of the basalt fibers used in the study was between 25–30 mm. The properties of basalt fiber are presented in Table 3.

2.2 Tests design

The content of SRA, the content of BF and RI were selected as the factors that influence the shrinkage performance. The roughness of interface was measured by the sand-filling method [33]. The experimental design scheme for the tests, including the levels of each factor, is presented in Table 4. There are nine groups with three specimens in each group.

2.3 Experimental procedures

The specimens used in the study were composed of two parts. First, a cuboid of old concrete, measuring 50 mm × 100 mm × 515 mm was poured. After 180 days, the surface of the old concrete part was artificially roughened. Then, a cuboid of new concrete, also measuring

Table 1 Concrete composition

Component	Cement	Water	Sand	Stone
Content (kg/m^3)	460	195	580	1165

Table 2 Technical data of cement

Weight of screen residue (%)	MgO (%)	SO_3 (%)	Initial setting time (min)	Final setting time (min)	Breaking strength (MPa)	Compressive strength (MPa)
1.75	3.60	1.8	150	210	8.1	49.5

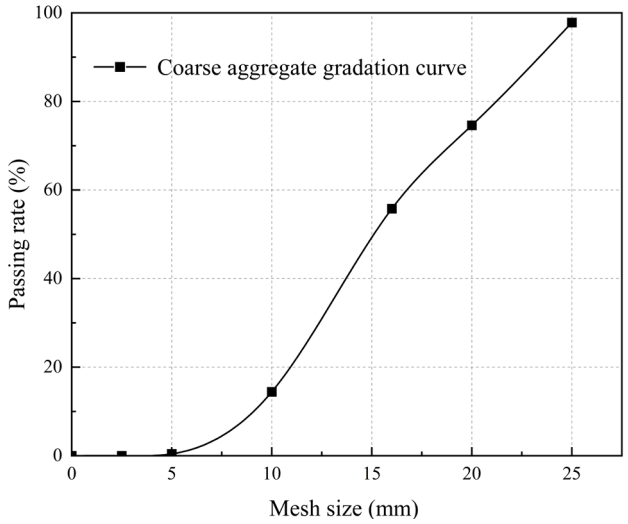

Fig. 1 Size distribution curves of aggregates

Table 3 Properties of basalt fiber

Density (kg/m^3)	Tensile strength (MPa)	Elasticity modulus (GPa)	Elongation (%)	Softening point (°C)
2870	3000~4840	79~93	3.1~3.2	960

50 mm × 100 mm × 515 mm was poured on top of the old concrete, as shown in Fig. 2. Shrinkage of the new concrete was measured using a non-contact shrinkage tester, as shown in Fig. 3. The basic principle is to fix the non-contact displacement sensor on the concrete, which can deform together with the concrete to determine the shrinkage of the concrete [34]. Each test lasted 30 days and was conducted with temperature of (20 ± 2) ℃, relative humidity (60 ± 5)%. In addition, a group of specimens was poured to measure free shrinkage, which had the same conditions as G3. The specimen was a cuboid of 50 mm × 100 mm × 515 mm.

2.4 Experimental results

The shrinkage behavior of each specimen was presented in Fig. 4, illustrating the progression of shrinkage over time. It was observed that the shrinkage exhibited rapid development in the early stage and a gradual increase in the later stage. Notably, the results of free shrinkage were found to be greater than those of G3, with G3 displaying the least shrinkage while G1 exhibited the highest shrinkage.

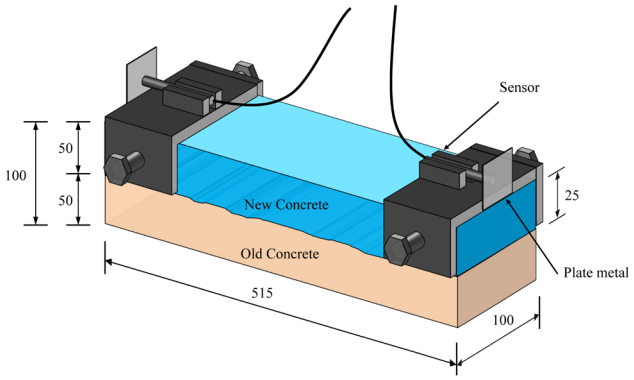

Fig. 2 Size of specimen (mm)

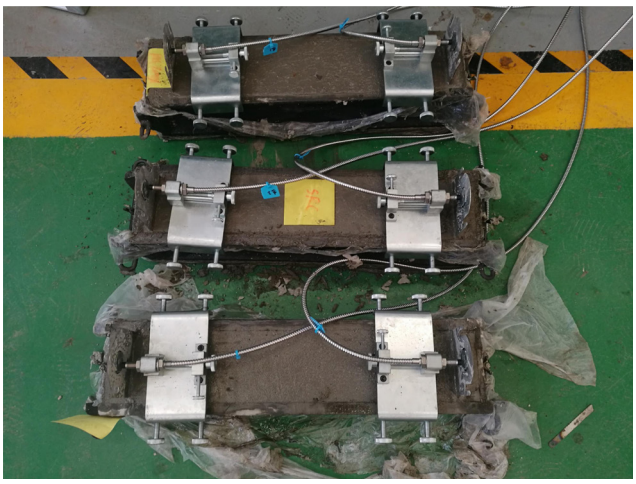

Fig. 3 Non-contact shrinkage test

It should be noted that a direct comparison of all specimens is not feasible. To illustrate this point, taking G6 and G8 as an example. Initially, the shrinkage strain of G8 was higher than that of G6. However, after a period of 10 days, the shrinkage value of G8 decreased to a lower level. This variation can be attributed to the difference in the SAR content between G8 and G6. Due to its lower SAR content, G8 initially experienced higher shrinkage strain compared to G6. Moreover, the RI of G8 was greater than that of G6, resulting in a lower shrinkage value after 10 days.

In summary, the results depicted in Fig. 4 highlight the varying shrinkage behavior among the different specimens. Further analysis and investigation are required to gain a comprehensive understanding of the underlying mechanisms driving these trends.

Table 4 Experimental conditions

Group	G1	G2	G3	G4	G5	G6	G7	G8	G9
SRA (%)	0	2	4	0	2	4	0	2	4
BF (kg/m^3)	0	3	6	3	6	0	6	0	3
RI (mm)	0.4~0.5	0.4~0.5	0.4~0.5	1.5~2.0	1.5~2.0	1.5~2.0	3.0~3.5	3.0~3.5	3.0~3.5

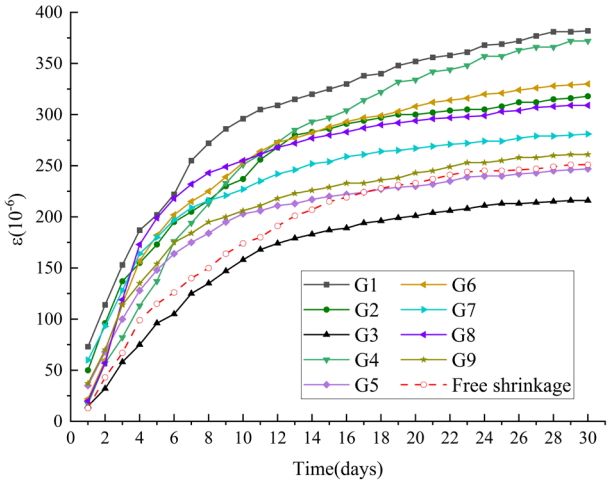

Fig. 4 Shrinkage test results

3 Restrained shrinkage mechanical model (RSMM)

After the old-new concrete specimen is formed, the new concrete will shrink, while the old concrete will not shrink as its shrinkage has already occurred. As a result, the shrinkage of new concrete is restrained by the old concrete. This creates a tension F_1 on the new concrete and a pressure F_2 on the old concrete, as shown in Fig. 5.

$$F_1(t) = -F_2(t) = -F(t) \tag{1}$$

It is an eccentric force for new or old concrete. The stresses of new concrete and old concrete are

$$\sigma_1(t) = \frac{F_1(t)}{A_1} + \frac{M_1(t)y_n}{I_1}, \tag{2}$$

$$\sigma_2(t) = \frac{F_2(t)}{A_2} + \frac{M_2(t)y_o}{I_2}. \tag{3}$$

Thus

$$\sigma_1(t) = \frac{F_1(t)}{A_1} + \frac{M_1(t)y_n}{I_1} = F_1(t)\left(\frac{1}{A_1} + \frac{y_1 y_n}{I_1}\right) = F_1(t)g_1, \tag{4}$$

$$\sigma_2(t) = \frac{F_2(t)}{A_2} + \frac{M_2(t)y_0}{I_2} = F_2(t)\left(\frac{1}{A_2} + \frac{y_2 y_o}{I_2}\right) = F_2(t)g_2, \tag{5}$$

where $F_1(t)$ indicates the force of old concrete on new concrete, $F_2(t)$ indicates the force of new concrete on old concrete. $\sigma_1(t)$ indicates the stress of new concrete section, $\sigma_2(t)$ indicates the stress of old concrete section. A_1, A_2 indicate the section area of old and new concrete. $M_1(t)$, $M_2(t)$ indicate the bending moments acting on new and old concrete. I_1, I_2 indicate the section moment of inertia of new and old concrete. y_1, y_2 indicate the distance between the force and the neutral axis of the new and old concrete. y_n indicates the distance from the stress checking point of new concrete to the neutral axis of new concrete, y_o indicates the distance from the stress checking point of old concrete to the neutral axis of old concrete.

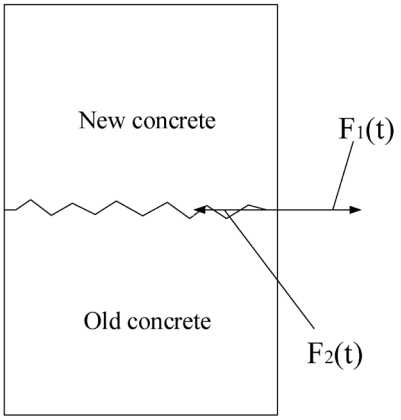

Fig. 5 Force of restrained shrinkage of new and old concrete

The shrinkage at time t is [35]

$$\varepsilon(t) = \frac{\sigma(t)}{E_c(t)}\left[1 + x(t,t_0)\varphi(t,t_0)\right] + \varepsilon_{\mathrm{sh}}(t), \tag{6}$$

where t_0 is initial loading time. $E_c(t)$ is the elasticity modulus of concrete at time t. $x(t,t_0)$ is the aging coefficient. $\varphi(t,t_0)$ is the creep coefficient. $\varepsilon_{sh}(t)$ is the free shrinkage of concrete at time t.

The deformation compatibility equation on the bonding interface between new and old concrete is [25]

$$\varepsilon_1(t) + \varepsilon_{\mathrm{nsh,t,t_0}}(t) = \varepsilon_2(t) + \varepsilon_{\mathrm{osh,t,t_0}}(t), \tag{7}$$

where $\varepsilon_1(t)$ is the shrinkage of new concrete. $\varepsilon_2(t)$ is the shrinkage of old concrete. $\varepsilon_{nsh,t,t_0}(t)$ is the free shrinkage of new concrete from t_0 to t. $\varepsilon_{osh,t,t_0}(t)$ is the free shrinkage of old concrete from t_0 to t. Then

$$\frac{F_1(t)g_1}{E_{28}}\left[1 + x_1(t,t_0)\right] + \varepsilon_{\mathrm{nsh,t,t_0}}(t) = \frac{F_2(t)g_2}{E_{28}}\left[1 + x_2(t,t_0)\varphi_2(t,t_0)\right] + \varepsilon_{\mathrm{osh,t,t_0}}(t)$$

Thus

$$F(t) = \frac{\left(\varepsilon_{\mathrm{nsh,t,t_0}}(t) - \varepsilon_{\mathrm{osh,t,t_0}}(t)\right)}{\frac{\left[1 + x_1(t,t_0)\varphi_1(t,t_0)\right]g_1}{E_{28}} + \frac{\left[1 + x_2(t,t_0)\varphi_2(t,t_0)\right]g_2}{E_{28}}}$$

Then according to Eq.(6), the shrinkage is

$$\varepsilon(t) = \frac{\left(\varepsilon_{\mathrm{nsh,t,t_0}}(t) - \varepsilon_{\mathrm{osh,t,t_0}}(t)\right)\left[1 + x_1(t,t_0)\varphi_1(t,t_0)\right]g_0}{\left[1 + x_1(t,t_0)\varphi_1(t,t_0)\right]g_1 + \left[1 + x_2(t,t_0)\varphi_2(t,t_0)\right]g_2} + \varepsilon_{\mathrm{sh}}(t) \tag{8}$$

If the geometric shape of new and old concrete is the same, $g_1 = g_2 = g$. And the free shrinkage of old concrete $\varepsilon_{osh,t,t_0}(t) = 0$, if the duration of old concrete is long enough. Then the Eq. (8) is simplified

$$\varepsilon(t) = \frac{\varepsilon_{\mathrm{nsh,t,t_0}}(t)\left[1 + x_1(t,t_0)\varphi_1(t,t_0)\right]}{2 + x_1(t,t_0)\varphi_1(t,t_0) + x_2(t,t_0)\varphi_2(t,t_0)} \frac{g_0}{g} + \varepsilon_{\mathrm{sh}}(t) \quad (9)$$

where, $g_0 = \left(\frac{1}{\mathrm{A_1}} + \frac{y_0 y_{\mathrm{n}}}{I_1}\right)$ is the distance from checking point to neutral axis of new concrete. This is the concrete restrained shrinkage mechanical model (RSMM).

4 Restrained shrinkage model based on the grey correlation analysis (RMGC)

4.1 Grey correlation analysis

Grey theory is a new approach to study problems with uncertain data and a lack of information [36, 37]. Grey correlation analysis (GCA) is an important part of grey theory, which determines the correlation of factors based on the similarity of the geometric shapes of sequence curves. GCA can solve the defects caused by using mathematical statistical methods for system analysis by introducing correlation in the analysis. The similarity of geometric shapes of sequence curves can be reflected by the grey correlation degree, which is a quantification of geometric shape similarity [38, 39]. This approach can be used to analyze complex systems with incomplete data and provide a more accurate understanding of the relationships between factors.

Assuming X_i is factor behavior sequence, Y_i is system characteristic behavior sequence. Operator D for normalizing sequences X_i, Y_i.

$$\begin{aligned} X_i' &= X_i D = \left(x_i(1)d, x_i(2)d, \ldots, x_i(m)d\right), \\ Y_j' &= Y_j D = \left(y_j(1)d, y_j(2)d, \ldots, y_j(m)d\right), \\ &\text{where} \\ x_i(k)d &= \frac{x_i(k)}{\frac{1}{m}\sum_{k=1}^{m} x_i(k)}; y_j(k)d = \frac{y_j(k)}{\frac{1}{m}\sum_{k=1}^{m} y_j(k)}, \\ k &= 1,2,\ldots,n. \end{aligned} \quad (10)$$

The steps to calculate the grey correlation degree are as follows [40, 41].

(1) Calculate the initial sequence of each sequence X_i', Y_j', (i = 1,2,…,n; j = 1,2,..h).

(2) Calculate interpolation sequences $\Delta i(k) = |Y_j'(k) X_i'(k)|$, ($k$ = 1,2,…, m)

(3) Calculate Maximum and Minimum

$$M = \max_i \max_k \Delta_i(k), N = \min_i \min_k \Delta_i(k)$$

(4) Calculate the correlation coefficient

$$\gamma_{ji}(k) = \frac{N + \xi M}{\Delta_i(k) + \xi M}, \xi \in (0,1)$$

where ξ is distinguishing coefficient. If ξ is smaller, the distinguishing ability is greater. In general case ξ = 0.5 [37]

(5) Calculate grey correlation degree

$$\gamma_{ji} = \frac{1}{m}\sum_{k=1}^{m} \gamma_{ji}(k), (i = 1,2,\ldots,n)$$

where m is number of samples and n is number of correlation factor sequences.

4.2 Hyperbolic shrinkage model

The shrinkage of new and old concrete after bonding has a hyperbolic correlation with time [42]. To describe this relationship, the bond shrinkage equation is assumed as [43].

$$\varepsilon(t) = At/(B + t), \quad (11)$$

where ε is the shrinkage of the old-new concrete. A, B are the fitting coefficients. t is the time after concrete initial-set. This equation describes the relationship between shrinkage and time, and it is commonly used to express the shrinkage behavior of bonded old-new concrete. The fitting results are shown in Fig. 6.

4.3 Modified formula based on the GCA

The values of the coefficients A and B in Eq. (11) are different for different experiments because the factors SRA, BF and RI are changed. The shrinkage of new and old concrete bonding is uncertain, so GCA can be used to find the important factors that affect the values of A and B. This simplifies the regression equation by reducing the number of variables and providing more accurate predictions of shrinkage.

The coefficient A and B can be considered as the system characteristic behavior sequence Y_j, and the factors SRA, BF and RI can be considered as the factor behavior sequence X_i. Then, the similarity of geometric shapes of the sequence curves of A and B can be compared with the sequence curves of the factors SRA, BF and RI.

$$\begin{aligned} A &= f(SRA, BF, RI), \\ B &= f(SRA, BF, RI). \end{aligned} \quad (12)$$

According to Eq. (12), the results of grey correlation degree are list in Table 5. And grey correlation parameters of rate plotted in Fig. 7.

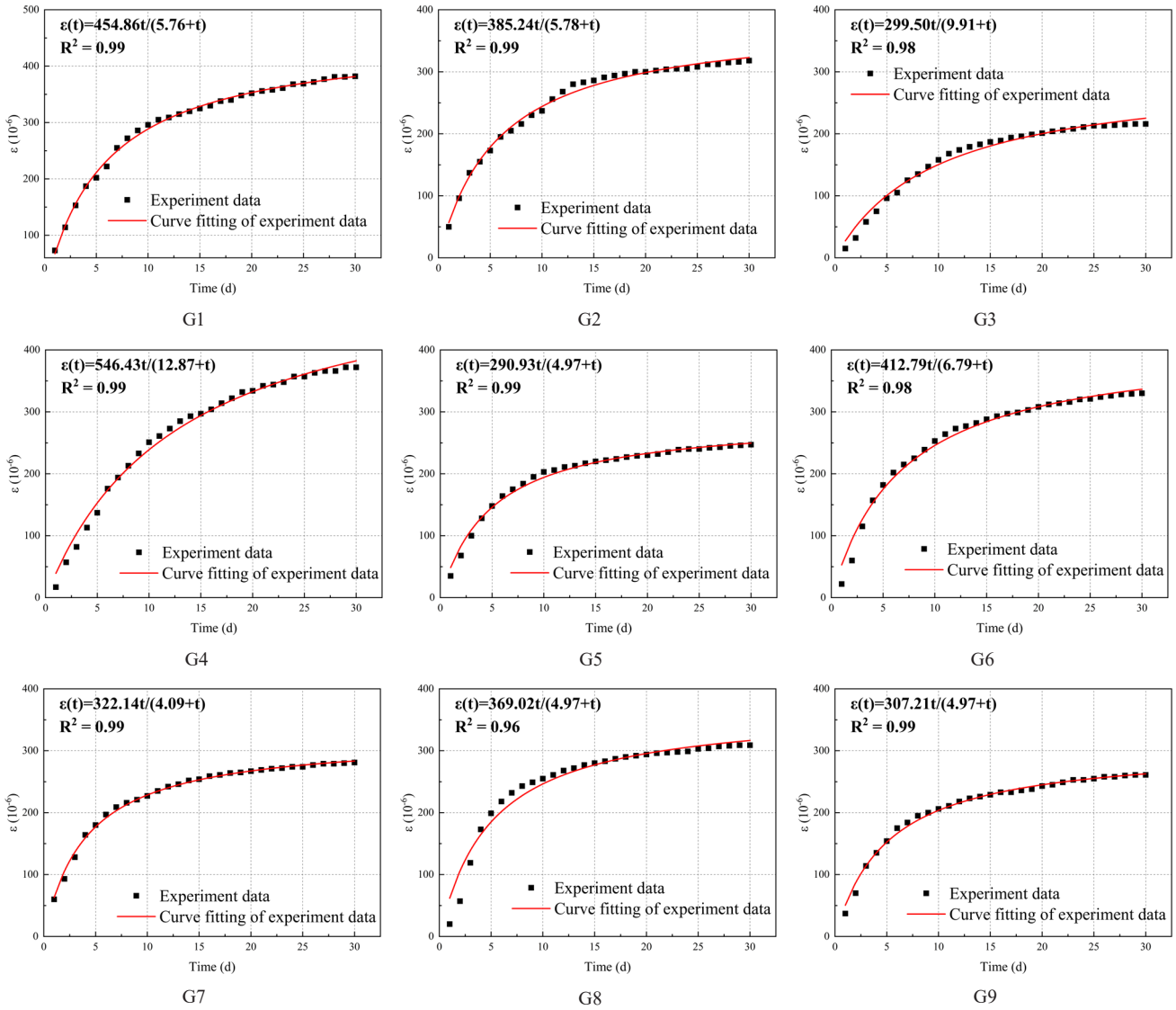

Fig. 6 Hyperbolic shrinkage model

Table 5 Results of grey correlation degree

Property	*A*	*B*
SRA	0.579	0.612
BF	0.538	0.614
RI	0.577	0.568

The results of the GCA analysis show that SRA and RI are important factors for coefficient *A*, while SRA and BF are important factors for coefficient *B*. In order to make the prediction equation as concise as possible, only the main factors are selected for fitting of coefficient *A* and *B*. Then, RMGC under the influence of SRA, BF, and RI can be established.

$$\mu(t)=\frac{\left(454.31-90.31SRA+69.13RI+10.52SRA^2-30.11RI^2+12.72SRA\times RI\right)t}{\left(7.91-2.85SRA+0.9BF+0.54SRA^2-0.2BF^2+0.2SRA\times BF\right)+t}. \quad (13)$$

According to Eq. (13), the comparison of the prediction results and test results on the 5th day, 15th day and 30th day are shown in Fig. 8. The coefficient of determination $R^2 = 0.8$, indicating that the fitting results have a high level of practical significance and accuracy.

5 Discussion

The concrete restrained shrinkage of G3 is calculated and plotted in Fig. 9. The results of the RSMM are closer to the test results, indicating that it is more accurate than the RMGC. RSMM has clear physical significance and rigorous logical reasoning, but it includes some factors and requires additional testing. On the other hand, RMGC is

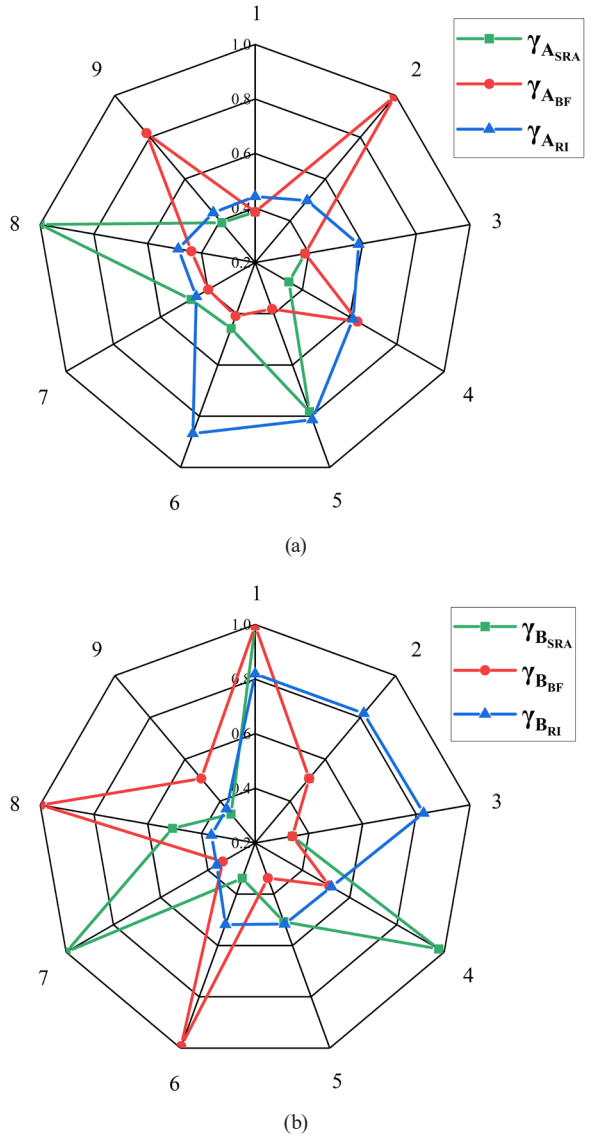

Fig. 7 Grey correlation parameters of rate of shrinkage: (a) γ_A, (b) γ_B

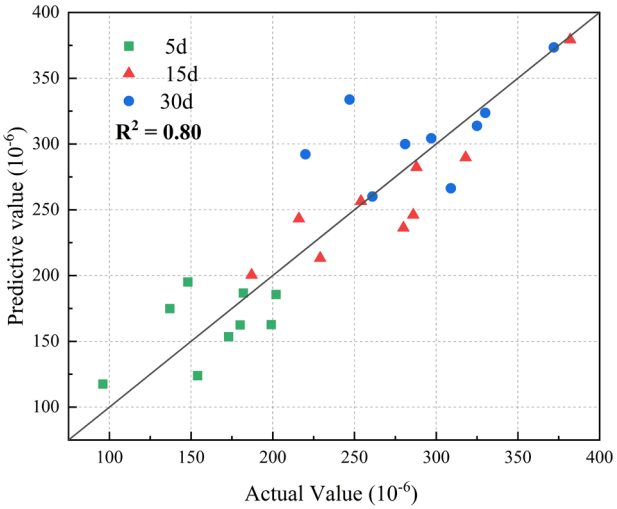

Fig. 8 Comparison of the prediction results and test results

based on existing data and is less restrictive, making it more effective and convenient to use. Thus, depending on the availability of data and resources, both RSMM and RMGC can be used to predict the shrinkage of new-to-old concrete, but RSMM is more accurate while RMGC is more convenient.

According to Eq. (12), the effects of SRA, BF and RI on shrinkage have been analyzed and plotted in Fig. 10. The results show that as SRA increases, the shrinkage decreases, and this is likely due to the shrinkage reducing admixtures' ability to slow down the concrete's shrinkage rate. The effect of BF on shrinkage is faint and it might have a minimal effect on the shrinkage. The effect of RI on shrinkage is varying and non-linear. With increase of RI, shrinkage undergoes first increase and then decrease. This is because, on one hand, the rougher the contact surface, the smaller the effective contact area, leading to a reduction in bonding force and shrinkage. On the other hand, the roughness of the contact surface increases, leading to an increase in the deformation resistance of the concrete, resulting in an increase in bonding force and shrinkage. So, within a certain range of RI, shrinkage decreases with the increase in roughness.

6 Conclusions

In this paper, an experimental study on the restraint-induced shrinkage behavior of the new-to-old concrete interface was carried out. RSMM and RMGC were proposed and discussed. The results of the experimental study were then compared against the predictions of both models to evaluate their accuracy and effectiveness. The following conclusions can be drawn.

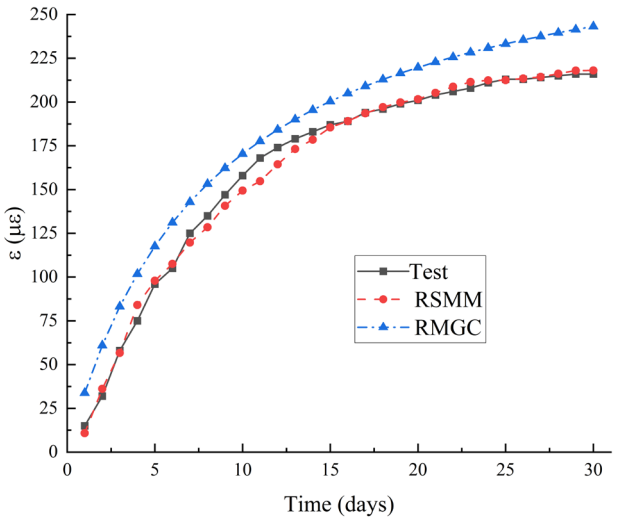

Fig. 9 Comparison of the prediction results and test results

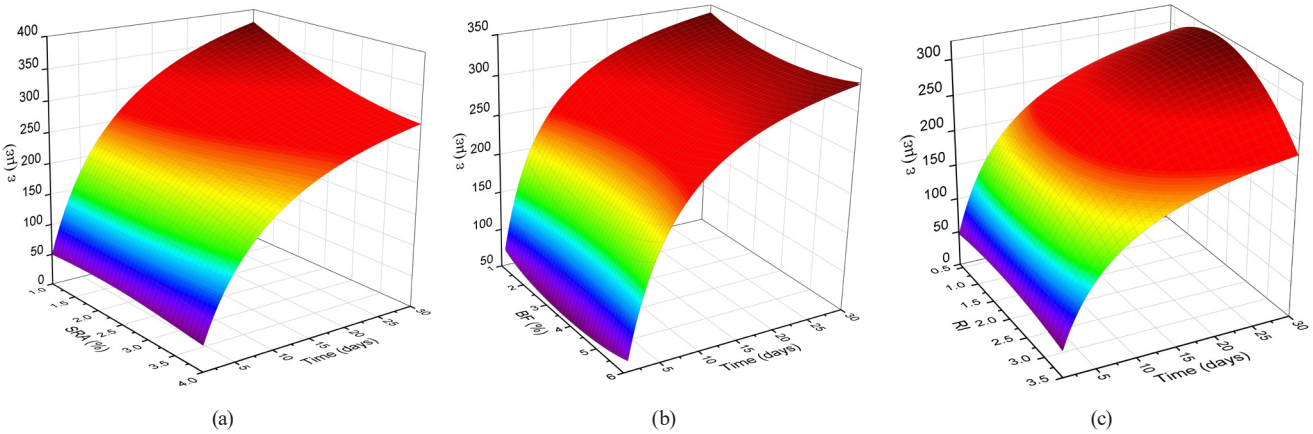

(a) (b) (c)

Fig. 10 Effect of SRA, BF and RI on shrinkage: (a) SRA (BF = 3%, RI = 1.5), (b) BF (SRA = 2%, RI = 1.5), (c) RI (SRA = 2%, BF = 3%)

1. The results obtained from RSMM were found to be more consistent with the experimental data, as compared to those obtained from RMGC. Additionally, RSMM has a clear physical interpretation and is supported by logical and rigorous reasoning. However, it should be noted that RSMM incorporates additional factors and further testing is required to fully validate its performance.
2. RMGC is a data-efficient approach that combines a hyperbolic shrinkage model with grey theory. It is specifically designed to work effectively with a limited number of data, making it less restrictive in terms of input requirements. This makes RMGC more effective and convenient when compared to other methods that may require larger datasets.
3. In RMGC, a data-efficient approach, considered SRA, BF and RI in its analysis. The results obtained from RMGC indicate that as the SRA and BF content increases, the shrinkage decreases. The quantitative analysis shows that the effect of the SRA was found to be more significant than that of the BF on reducing shrinkage. Additionally, the results reveal that as the RI value increases, shrinkage initially increases but then reaches a minimum value beyond a certain threshold of RI. This behavior can be explained by the combined effects of SRA, BF and RI on concrete shrinkage.

Acknowledgement

This work is supported by the Liaoning Provincial Natural Science Foundation Guidance Projects (2019-ZD-0006).

Conflicts of Interest

The authors declare no conflict of interest.

References

[1] Zhou, A., Qin, R., Feo, L., Penna, R., Lau, D. "Investigation on interfacial defect criticality of FRP-bonded concrete beams", Composites Part B: Engineering, 113, pp. 80–90, 2017. https://doi.org/10.1016/j.compositesb.2016.12.055

[2] Beushausen, H., Alexander, M. G. "Failure mechanisms and tensile relaxation of bonded concrete overlays subjected to differential shrinkage", Cement and Concrete Research, 36, pp. 1908–1914, 2006. https://doi.org/10.1016/j.cemconres.2006.05.027

[3] Beushausen, H., Bester, N. "The influence of curing on restrained shrinkage cracking of bonded concrete overlays", Cement and Concrete Research, 87, pp. 87–96, 2016. https://doi.org/10.1016/j.cemconres.2016.05.007

[4] Wu, D., Gao, W., Feng, J., Luo, K. "Structural behaviour evolution of composite steel-concrete curved structure with uncertain creep and shrinkage effects", Composites Part B: Engineering, 86, pp. 261–272, 2016. https://doi.org/10.1016/j.compositesb.2015.10.004

[5] Neubauer, C. M., Jennings, H. M., Garboczi, E. J. "Mapping drying shrinkage deformations in cement-based materials", Cement and Concrete Research, 27(10), pp. 1603–1612, 1997. https://doi.org/10.1016/S0008-8846(97)00217-2

[6] Zhang, W., Lin, H., Xue, M., Wang, S., Ran, J., Su, F., Zhu, J. "Influence of shrinkage reducing admixtures on the performance of cementitious composites: A review", Construction and Building Materials, 325, 126579, 2022. https://doi.org/10.1016/j.conbuildmat.2022.126579

[7] Hasholt, M. T., Jensen, O. M. "Chloride migration in concrete with superabsorbent polymers", Cement and Concrete Composites, 55, pp. 290–297, 2015. https://doi.org/10.1016/j.cemconcomp.2014.09.023

[8] Mechtcherine, V., Secrieru, E., Schröfl, C. "Effect of superabsorbent polymers (SAPs) on rheological properties of fresh cement-based mortars - Development of yield stress and plastic viscosity over time", Cement and Concrete Research, 67, pp. 52–65, 2015. https://doi.org/10.1016/j.cemconres.2014.07.003

[9] He, Y., Zhang, X., Hooton, R. D., Zhang, X. "Effects of interface roughness and interface adhesion on new-to-old concrete bonding", Construction and Building Materials, 151, pp. 582–590, 2017. https://doi.org/10.1016/j.conbuildmat.2017.05.049

[10] Fan, J., Wu, L., Zhang, B. "Influence of Old Concrete Age, Interface Roughness and Freeze-Thawing Attack on New-to-Old Concrete Structure", Materials, 14(5), 1057, 2021. https://doi.org/10.3390/ma14051057

[11] Maili, C., Jing, M. "Experimental Study on Shear Behavior of the Interface between New and Old Concrete with Reinforced", KSCE Journal of Civil Engineering, 22, pp. 1882–1888, 2018. https://doi.org/10.1007/s12205-017-2007-6

[12] Zhang, X., Zhang, W., Luo, Y., Wang, L., Peng, J., Zhang, J. "Interface Shear Strength between Self-Compacting Concrete and Carbonated Concrete", Journal of Materials in Civil Engineering, 32(6), 04020113, 2020. https://doi.org/10.1061/(ASCE)MT.1943-5533.0003229

[13] Liang, Y., Lei, Z., Dong, L., Bo, C. "Shear test of the rectangular beam on the new to old concrete interface based on Digital Image Correlation", IOP Conf. Series: Earth and Environmental Science, 267, 032058, 2019. https://doi.org/10.1088/1755-1315/267/3/032058

[14] Courard, L., Piotrowski, T., Garbacz, A. "Near-to-surface properties affecting bond strength in concrete repair", Cement and Concrete Composites, 46, pp. 73–80, 2014. https://doi.org/10.1016/j.cemconcomp.2013.11.005

[15] Ran, Q., Gao, N., Liu, J., Tian, Q., Zhang, J. "Shrinkage action mechanism of shrinkage-reducing admixtures based on the pore solution", Magazine of Concrete Research, 65, pp. 1092–1100, 2013. https://doi.org/10.1680/macr.12.00224

[16] Palacios, M., Puertas, F. "Effect of shrinkage-reducing admixtures on the properties of alkali-activated slag mortars and pastes", Cement and Concrete Research, 37(5), pp. 691–702, 2007. https://doi.org/10.1016/j.cemconres.2006.11.021

[17] Rajabipour, F., Sant, G., Weiss, J. "Interactions between shrinkage reducing admixtures (SRA) and cement paste's pore solution", Cement and Concrete Research, 38(5), pp. 606–615, 2008. https://doi.org/10.1016/j.cemconres.2007.12.005

[18] Zhan, P., He, Z. "Application of shrinkage reducing admixture in concrete: A review", Construction and Building Materials, 201, pp. 676–690, 2019. https://doi.org/10.1016/j.conbuildmat.2018.12.209

[19] Rahman, M., Chen, Y., Ibrahim, A., Lindquist, W., Tobias, D., Krstulovich, J., González, D., Hindi, R. "Study of Drying Shrinkage Mitigating Concrete Using Scaled Bridge Bays", International Journal of Civil Engineering, 18(1), pp. 65–73, 2020. https://doi.org/10.1007/s40999-019-00460-z

[20] Folliard, K. J., Berke, N. S. "Properties of high-performance concrete containing shrinkage-reducing admixture", Cement and Concrete Research, 27(9), pp. 1357–1364, 1997. https://doi.org/10.1016/S0008-8846(97)00135-X

[21] Qin, R., Hao, H., Rousakis, T., Lau, D. "Effect of shrinkage reducing admixture on new-to-old concrete interface", Composites Part B: Engineering, 167, pp. 346–355, 2019. https://doi.org/10.1016/j.compositesb.2018.11.087

[22] Bouziadi, F., Boulekbache, B., Hamrat, M. "The effects of fibres on the shrinkage of high-strength concrete under various curing temperatures", Construction and Building Materials, 114, pp. 40–48, 2016. https://doi.org/10.1016/j.conbuildmat.2016.03.164

[23] Gong, J., Ma, Y., Fu, J., Hu, J., Ouyang, X., Zhang, Z., Wang H. "Utilization of fibers in ultra-high performance concrete: A review", Composites Part B: Engineering, 241, 109995, 2022. https://doi.org/10.1016/j.compositesb.2022.109995

[24] Statkauskas, M., Grinys, A., Vaičiukynienė, D. "Investigation of Concrete Shrinkage Reducing Additives", Materials, 15, 3407, 2022. https://doi.org/10.3390/ma15093407

[25] Cheng, H. Q., Ga, D. Y. "Shrinkage Performance of Adherence of New Steel Fiber-Reinforced Concrete to Old Concrete", Advanced Materials Research, 163–167, pp. 3569–3574, 2011. https://doi.org/10.4028/www.scientific.net/AMR.163-167.3569

[26] Yousefieh, N., Joshaghani, A., Hajibandeh, E., Shekarchi, M. "Influence of fibers on drying shrinkage in restrained concrete", Construction and Building Materials, 148, pp. 833–845, 2017. https://doi.org/10.1016/j.conbuildmat.2017.05.093

[27] Papp, D., Orban, Z. "Effects of sub-base surface roughness on shrinkage cracking of industrial floors", Pollack Periodica, 13, pp. 57–64, 2018. https://doi.org/10.1556/606.2018.13.1.5

[28] Santos, P. M. D., Júlio, E. N. B. S. "Factors Affecting Bond between New and Old Concrete", ACI Materials Journal, 108(4), pp. 449–456, 2011. https://doi.org/10.14359/51683118

[29] Lampropoulos, A., Dritsos, S. "Concrete Shrinkage Effect on Columns Strengthened with Concrete Jackets", Structural Engineering International, 20, pp. 234–239, 2010. https://doi.org/10.2749/101686610792016781

[30] Wang, W., Dai, J., Li, G., Huang, C. "Long-Term Behavior of Prestressed Old-New Concrete Composite Beams", Journal of Bridge Engineering, 16(2), pp. 275–285, 2011. https://doi.org/10.1061/(ASCE)BE.1943-5592.0000152

[31] Bernard, O., Brühwiler, E. "Influence of autogenous shrinkage on early age behaviour of structural elements consisting of concretes of different ages", Materials and Structures, 35, pp. 550–556, 2002. https://doi.org/10.1007/BF02483123

[32] Farzad, M., Shafieifar, M., Azizinamini, A. "Experimental and numerical study on bond strength between conventional concrete and Ultra High-Performance Concrete (UHPC)", Engineering Structures, 186, pp. 297–305, 2019. https://doi.org/10.1016/j.engstruct.2019.02.030

[33] Dong, W., Wu, Z., Zhou, X. "Fracture Mechanisms of Rock-Concrete Interface: Experimental and Numerical", Journal of Engineering Mechanics, 142(7), 04016040, 2016. https://doi.org/10.1061/(ASCE)EM.1943-7889.0001099

[34] Shang, M., Qiao, H., He, Z., Zhang, Y., Liu, X., Zhang, Y., Wang, J. "Study on the shrinkage mechanism and prediction model of high-strength specified density concrete based on the internal curing micro-pump effect of MSW incineration tailings", Construction and Building Materials, 372, 130804, 2023. https://doi.org/10.1016/j.conbuildmat.2023.130804

[35] Au, F. T. K., Liu, C. H., Lee, P. K. K. "Creep and shrinkage analysis of reinforced concrete frames by history-adjusted and shrinkage-adjusted elasticity moduli", The Structural Design of Tall and Special Buildings, 18(1), pp. 13–35, 2009.
https://doi.org/10.1002/tal.391

[36] Liu, S., Forrest, J. Y. L., Yang, Y. "Grey System: Thinking, Methods, and Models with Applications", In: Zhou, M., Li, H.-X., Weijnen, M. (eds.) Contemporary Issues in Systems Science and Engineering, Wiley, 2015, pp. 153–224. ISBN:9781118271865
https://doi.org/10.1002/9781119036821.ch4

[37] Liu, S., Yang, Y., Forrest J. "Grey Incidence Analysis Models", In: Grey Data Analysis, Springer, 2017, pp. 67–103. ISBN: 978-981-10-9458-3
https://doi.org/10.1007/978-981-10-1841-1_5

[38] Liu, S., Lin, Y. "Grey Models for Decision Making", In: Grey Systems, Springer, 2011, pp. 197–223. ISBN: 978-3-642-42332-1
https://doi.org/10.1007/978-3-642-16158-2_7

[39] Kumar, S., Mitra, B., Kumar, N. "Application of GRA method for multi-objective optimization of roller burnishing process parameters using a carbide tool on high carbon steel (AISI-1040)", Grey Systems: Theory and Application, 9(4), pp. 449–463, 2019.
https://doi.org/10.1108/GS-03-2019-0006

[40] Wu, H., Lei, H., Chen, Y. F. "Grey relational analysis of static tensile properties of structural steel subjected to urban industrial atmospheric corrosion and accelerated corrosion", Construction and Building Materials, 315, 125706, 2022.
https://doi.org/10.1016/j.conbuildmat.2021.125706

[41] Zhu, L., Zhao, C., Dai, J. "Prediction of compressive strength of recycled aggregate concrete based on gray correlation analysis", Construction and Building Materials, 273, 121750, 2021.
https://doi.org/10.1016/j.conbuildmat.2020.121750

[42] Nguyen, V. C., Tong, F. G., Nguyen, V. N. "Modeling of autogenous volume deformation process of RCC mixed with MgO based on concrete expansion experiment", Construction and Building Materials, 210, pp. 650–659, 2019.
https://doi.org/10.1016/j.conbuildmat.2019.03.226

[43] Gribniak, V., Kaklauskas, G., Bacinskas, D. "Shrinkage in reinforced concrete structures: A computational aspect", Journal of Civil Engineering and Management, 14(1), pp. 49–60, 2008.
https://doi.org/10.3846/1392-3730.2008.14.49-60